Smart bandage dyed with sensor probe encapsulated in alginate for wound healing monitoring

Tawfik A. Khattab[1,*], Ahmed Mohamed Farok Ahmed[2] and Nesreen Awad El-Nakib[3]

[1]Dyeing, Printing and Auxiliaries Department, Textile Industries Research Division, National Research Centre, 33 El-Buhouth Street, Dokki, Cairo 12622, Egypt.

[2]Home Economics, Faculty of Specific Education, Fayum University, Egypt; Email: ahmedfarok15@gmail.com

[3]Home Economics (Clothes and Textile) Women's College, Ain Shams University, Egypt; Email: nana_fashion2000@yahoo.com

(*) Corresponding author: Dr. Tawfik Khattab (ta.khattab@nrc.sci.eg)

Abstract

Novel *in-situ* dressing bandage-based disposable probe that changes color upon wound healing was developed. Developing colorimetric technical textile pH-sensor can lead to attractive end-use applications as it represents the potential for inexpensive, fast, flexible pH-sensors. Herein we describe the preparation of tricyanofuran-hydrazone based disperse colorant to act as a color changeable pH-sensor. The pH responsive tricyanofuran-hydrazone was encapsulated as a core material in Ca-alginate microcapsule as a wall-former, which was loaded onto a cotton gauze by padding. This reversible color change depending on pH variations was due to charge delocalization of tricyanofuran-hydrazone anion form generated that led to a quinoid-type molecular switching. This tricyanofuran-hydrazone colorant was employed for use in technical textile materials with a pH sensing capability. The approach adopted in the present study was based on dyeing of cotton gauze using tricyanofuran-hydrazone that can afford numerical results for the pH of the wound fluid. The dyed gauze matrix showed a clear reversible color change upon exposure to acid-base solutions as indicated by color coordinates. Our results indicate an obvious color change shown to the naked eye, from orange to purple, which can be recognized at the surface of the employed fabrics when exposed to basic conditions. The surface morphology of the treated cotton gauze was investigated under scanning electron microscopy, energy-dispersive X-ray, and mapping. The treated cotton gauze was studied by exploring of the air-permeability, stiffness, and colorfastness.

Keywords: Hydrazone; Disperse colorant**;** Cotton gauze; Smart bandage; Wound healing.

1. Introduction

Smart textiles can be considered as a growing research field especially for the colorimetric technical textile-based sensors that can change colors in response to external changes including pH, light, electricity and solvent polarity [1-5]. The physicomechanical properties of textiles make them preferred solid state matrices for immobilizing a variety of substances. The advantages of textile sensors derived from their large surface area and high-quality mechanical and exploitation characteristics such as flexibility, softness, strength, lightness, and capability to permeate fluids and gases [6-11]. The large contact surface of textile fabrics usually allows efficient contact with the detected targeted substance compared to other polymers employed for similar purposes. The interaction between the dye and the fabric may inhibit the dye molecular sensing and color variations that can be observed in the solution state. Research on the application and immobilization of chromic colorants into textiles via conventional dyeing procedures is limited [12-15].

Slow healing injuries and their treatment have been a substantial difficulty for health care practitioners. Monitoring pH of an injury has been the spotlight of several recent investigations as the pH changes at the injury location can afford practical information regarding wounds evolution [16-19]. The pH of healthy skins is acidic to some extent (pH in the range of 5.0-5.5). On the other hand, the wounded skins, particularly infected one, demonstrate either neutral or slightly basic conditions (pH in the range of 7.0-8.5) as a result of the existence of different kinds of enzymes and/or bacteria [20-28]. This strongly suggests a direct relationship between skin pH and wound healing. Consequently, it is supposed that different pH values can advantage wound healing/infection at different stages, but the lack of appropriate techniques that can offer enough information on wound healing/infection is still a major limitation [29-33]. Herein, we develop a novel *in-situ* halochromic technical textile-based disposable probe that can address the above concerns and which can be employed as a simple and strong tool in the clinician's armory. Using colorimetric approach for wound healing monitoring is a helpful diagnostic tool due to the benefit of being non-invasive, simple, introduce real-time detection results, flexible, comfortable, high porosity and high surface area, no need for complicated instrumentations or trained personnel, simple operation and easy processing. The approach adopted in the present study was based on dyeing of cotton gauze using tricyanofuran-hydrazone dye sensor. This bandage-based disposable pH sensor for potential monitoring of wound healing/infection by introducing immediate visible signal was described.

2. Experimental details

2.1. Preparation of hydrazone probe

The hydrazone-based dye sensor was prepared by stirring 2,4-dinitro-5-fluoroaniline (3 mmol) and hydrochloric acid (20 mL) on a magnetic stirrer at 0-5ºC. An aqueous solution of sodium nitrite (3 mmol) in was then added slowly to afford the corresponding diazonium salt, which was added slowly to a mixture of tricyanofuran (3 mmol) and sodium acetate (5 g) in acetone (20 mL) at 0-5ºC with vigorous stirring. The product was filtered off, washed with distilled water, recrystallized from a mixture of ethanol to give a red powder (yield 62%); mp 225-227°C; ^{1}H-NMR (400 MHz, DMSO-d_6): 12.32 (singlet-broad, 1 H, N-H), 8.60 (singlet-broad, 1 H *aliphatic*, =C-H), 8.45 (doublet, *J*= 8.0 Hz, 1 H aromatic), 7.62 (doublet, *J*= 8.0 Hz, 1 H *aromatic*), 1.79 (singlet, 6 H *aliphatic*); ^{13}C-NMR (400 MHz, DMSO-d_6): 177.56, 172.94, 158.52, 136.99, 125.07, 118.47, 115.76, 113.63, 113.78, 112.14, 99.85, 98.02, 55.43, 26.75, 23.93; IR (neat, ν/cm^{-1}): 3285 (for secondary amine group), 2203 (for cyanide group), 1584 (for C=N group), 1505 and 1330 (for nitro groups). MS *m/z* (%): 410 [*M*-H]$^{+}$. Elemental analysis for hydrazone-based dye ($C_{17}H_{10}FN_7O_5$; 411.07): *calculated* C 49.64, H 2.45, F 4.62, N 23.84; *found* C 49.51, H 2.28, F 4.69, N 23.76

2.2. Preparation of cotton gauze sensor

Sodium alginate (1wt%) and hydrazone-based dye sensor (0.5, 1, 1.5, 2 and 2.5wt%) dissolved in 2-5mL acetone, were added to distilled water (50 mL). Cotton gauze were padded in the prepared solutions for 10 min. followed by padding in a calcium chloride aqueous solution (1 mM) for 10 min. The treated cotton gauze was washed with running water and finally air-dried.

2.3. Materials and apparatus

Melting point of hydrazone-based dye was obtained uncorrected (^{o}C) on Stuart SMP30. NMR spectrum was explored on BRUKER-AVANCE 400 spectrometer at 400 MHz. FTIR spectrum of the prepared hydrazone-based dye was recorded on Nexus-670 (Nicolet, United States). Elemental analysis was performed on PerkinElmer-2400 (Norwalk, United States). Mass spectrum was measured on Shimadzu GCMS-QP-1000-EX spectrometer. Scanning electron microscope (SEM) with a Quanta FEG-250 (Czech Republic) connected to energy-dispersive X-ray analysis (TEAM-EDAX) was applied to study both

morphology and elemental content. The pH was monitored by BECKMAN-COULTER pHI340. The calcium alginate microparticle diameter was measured by SEM Image J software. The color changes were reported on Texflach ACS/Datacolor with a Spectral flash 600 spectrophotometer. The color data were explored by studying CIE L*, a^*, and b^* coordinates. The colorfastness properties were examined according to ISO standards; ISO 105-X12(1987) for rubbing; ISO 105-E04(1989) for perspiration, ISO 105-B02(1988) for light, and ISO 105-C02(1989) for washing.

Cotton (100%) Medical Gauze Bandage 1.ISO,CE made from 40s cotton yarns white gauze, mesh 19*15 was employed in this study. The cotton gauze was desized, scoured, and bleached according to previously reported literature procedures [34]. Sodium alginate and calcium chloride were obtained from Sigma-Aldrich. Tricyanofuran as a starting material and hydrazone-based dye sensor were prepared according to previous literature synthetic methods [35], in which tricyanofuran and hydrazone-based dye were re-crystallized and obtained in high purity using flash column chromatography and reactions were visually monitored by TLC (PF254) under ultraviolet lamp (365nm).

2.4. Cotton gauze sensing exploration

The pH of a distilled water solution was changed by adding (C□H□)□N-OH to increase the pH value to alkaline or adding CF□COOH to decrease the pH value to acidic The prepared solutions at different pH values (between 5 and 8.5) were sprayed on the cotton gauze to show an instant color shifting from orange to purple.

3. Results and Discussion

3.1. Preparation of smart bandage

Hydrazone-based sensors have been known as multi-stimuli responsive molecular switches to pH and temperature. They have been used as solution probes and as solid state sensors in polymer matrices for pH monitoring, and detection of ammonia and amines. The tricyanofuran **1** starting material bearing an active-methyl was simply prepared depending previous literature procedure [35]. The hydrazone sensor probe **2** was prepared via azo-coupling reaction of the heterocyclic compound and the diazonium salt of 2,4-dinitro-5-fluoroaniline (Scheme **1**). The hydrazone chromophore was characterized by ^{1}H- and ^{13}C-NMR spectroscopy, mass, elemental analysis, and FTIR spectroscopy.

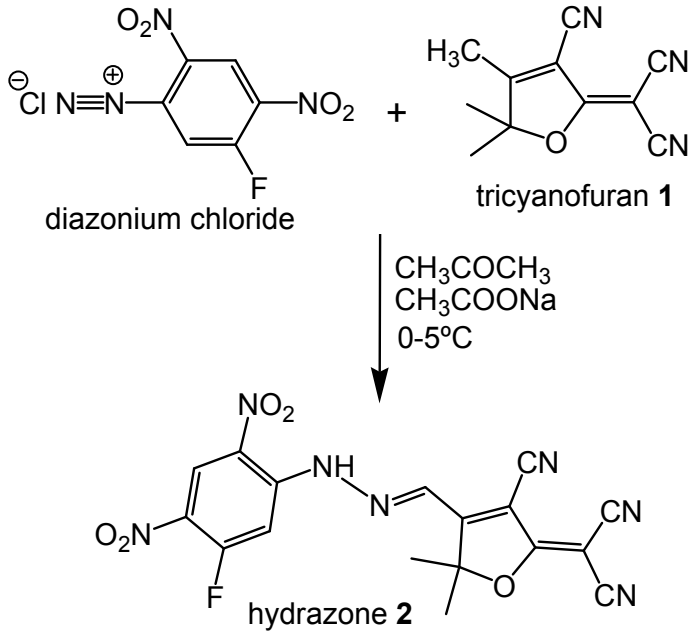

Scheme 1: Preparation of the hydrazone-based sensor chromophore.

The mechanism of wound healing monitoring depended mainly on the protonation-deprotonation reversible effect of the hydrazone sensor dye **2** (Scheme **2**) which was integrated within Ca-alginate microcapsules on cotton gauze.

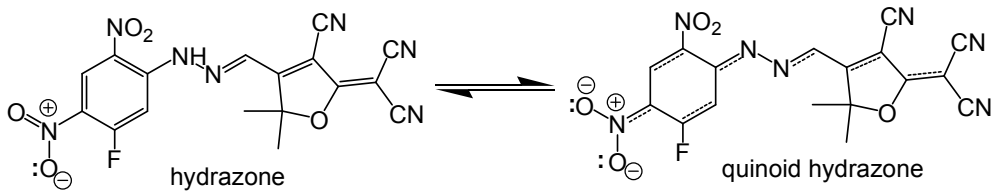

Scheme 2: Proposed mechanism of hydrazone sensor dye protonation-deprotonation reversibility.

The sensor microcapsules were assembled by concurrent co-precipitation of Na-alginate and the hydrazone chromophore into crosslinked Ca-alginate enclosing the hydrazone dye as dispersed active sites through the alginate matrix. Gauze samples were immersed in an aqueous solution of Na-alginate and hydrazone dye sensor, and then air-dried followed by immersion in an aqueous solution of $CaCl_2$ to commence the crosslinking operation. Upon adding Na-alginate into a solution of $CaCl_2$, the divalent Ca^{++} replaced the monovalent Na^{+} in the

alginate polymer chains. Each monovalent Na^{+} can be bonded to one polymer strand, while each divalent Ca^{++} can be crosslinked to two polymer strands. Alginate is a polysaccharide that has been applied in foodstuffs, pharmaceutical and dental purposes, thickeners, stabilizing and gelling agents, and wound dressings. Five different solutions were prepared depending on the hydrazone dye concentration in distilled water (0.5, 1, 1.5, 2 and 2.5wt%).

3.2. Morphological properties

The morphological properties and elemental composition of the treated cotton gauze surface integrated with Ca-alginate microcapsules which was molecularly imprinted by hydrazone-based dye were explored (Figure **1**). The scanning electron microscope images of the padded cotton gauze demonstrated successful coating of cotton surface with clusters of Ca-alginate microcapsules displaying nano/microstructures of irregular shapes. The size-distribution of the obtained nano/microstructured Ca-alginate microcapsules on cotton fabric surface was in the range from ~400nm to ~6μm. The main size average of the Ca-alginate microcapsules was about ~3μm. Such nano/microstructural Ca-alginate microcapsules tended to agglomerate, and accordingly dispersed slightly heterogeneous onto the cotton gauze, which could be assigned to the sort of chemical or physical interactions of the Ca-alginate macromolecules with the cotton gauze. Furthermore, the scanning electron microscope images demonstrated no physical changes happened to the surface of the treated cotton gauze.

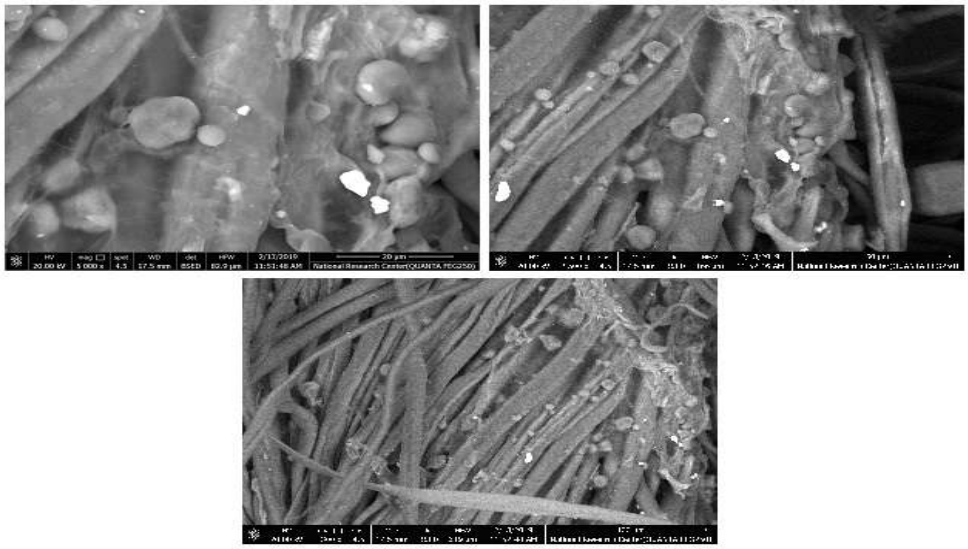

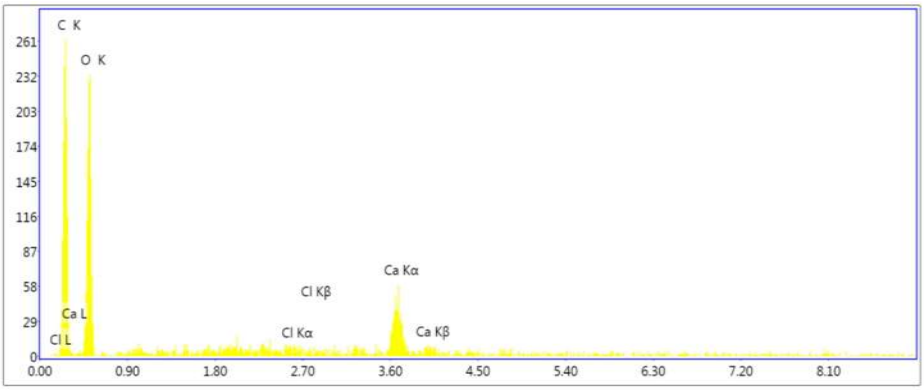

Figure 1: SEM *(top)* and EDAX (*bottom*) of treated cotton gauze (Sample 1.5wt%).

Table 1: Elemental content (weight %) at two different spots of treated cotton gauze (Sample 1.5wt%).

Sample spot	Carbon	Oxygen	Calcium	Chlorine
Spot 1	50.29	43.34	5.10	1.27
Spot 2	50.33	43.38	5.25	1.04

The elemental composition of the treated cotton gauze was also explored by EDAX spectroscopic analysis via measuring the elemental weight percent at two different spots on the treated cotton gauze surface as shown in Table **1**. The elemental contents picked at those two scanned spots were closely the same. This proved the homogenous immobilization of Ca-alginate microcapsules on cotton gauze surface. The mapping diagram of the key elements confirmed the uniform distribution of the Ca-alginate microcapsules on the surface of the treated cotton gauze. The Ca-alginate microcapsules were embedded onto cotton gauze to introduce porous three-dimensional scaffolds bearing large surface area and high porosity. Thus, the solid-state cotton gauze sensor demonstrated high sensitivity toward pH changes as a result of the high surface-to-volume ratio and large porous structural design, which facilitate the diffusion of the guest wound fluid within Ca-alginate microcapsules integrated within the cotton gauze matrix.

3.3. Color coordinates changes with wound healing

Determining the pH of a wound can supply information about the healing process and the occurrence of infection. Wound pH is not usually measured, but can be ascertained simply using the cotton gauze matrix loaded with Ca-alginate which in turn was activated with hydrazone sensor dye. A bandage capable of detecting pH would represent non-invasive and instant information about a wound to help

medical treatment. Experiments were conducted to evaluate the potential of the hydrazone-based dye as a pH-sensitive dye that can be used to color cotton gauze sensor bandage toward a wound mimic solution at different pH values. Changes in gauze color were observed by comparing the color coordinates L^*, a^*, b^* values before and after the smart bandage were exposed to the wound mimic solution. The cotton gauze sensor was integrated with hydrazone-based dye sensor immobilized within Ca-alginate microcapsules. The instantaneous color change was visually recognized from orange to purple depending on the pH value. The three dimensional color coordinates L^*, a^*, b^* of the smart cotton gauze samples treated at different concentrations of hydrazone-based dye sensor before and after exposure to wound mimic solution were displayed in Table **2.** The lightness/darkness was represented by L^*, green/red was represented by a^*, and blue/yellow represented by b^*. The treated cotton gauze samples possessed orange color, while the blank untreated cotton possessed white color (L^*= 95.23, a^*= 0.04, b^*= -1.28). The exposure of treated cotton gauze samples to wound mimic solution led to an increase in the maximum absorbance wavelength of cotton gauze from 450 to 535nm. The color coordinates (L^*, a^*, b^*) of the Ca-alginate microcapsules incorporated on cotton gauze were recorded before and after exposure to wound mimic solution. Depending on the concentration of the hydrazone-based dye sensor, all treated cotton gauze samples, before and after exposure to wound mimic solution, showed considerably dissimilar L^*, a^* and b^* magnitudes comparative to the pristine cotton. For both conditions, before and after exposure to wound mimic solution, L^* was comparatively decreased with increasing the hydrazone-based dye sensor concentration from 0.5-2.5%. However, a considerable increase was monitored in L^*, mostly for the hydrazone-based dye sensor concentration at 1.5wt%, after exposure to wound mimic solution to signify darker shade. Before exposure to wound mimic solution, the increased a^* and decreased b^* positive values indicated orange shade of all treated cotton gauze samples at all hydrazone-based dye concentrations. After exposure to wound mimic solution, the increased positive a^* and negative b^* values indicated purple shade of all treated cotton gauze samples. For all samples, after exposure to wound mimic solution, a^* positive magnitudes were positively increased to designate more red, while positive b^* magnitudes were changed to negative to designate more purple.

Table 2. Color coordinates of Ca-alginate microcapsules incorporated on cotton gauze with different concentrations of hydrazone-based sensor; before and after exposure to wound mimic solution.

Dye wt%	L*		a*		b*	
	before	after	before	after	before	after
0.5	67.09	45.20	5.00	7.25	15.22	- 7.54
1.0	67.29	43.92	8.64	9.62	12.83	- 8.78
1.5	65.67	33.25	9.06	10.52	9.28	- 12.08
2.0	64.37	32.44	10.74	12.65	7.46	- 13.77
2.5	62.02	30.72	12.19	12.54	4.21	- 16.80

3.4. Stiffness and comfort performance

The major reason of applying the padding technique was to establish a smooth fabric surface with low film thickness and low roughness, while keeping the cotton fabric's flexibility and air-permeability. Shirley Stiffness Tester was employed to measure the bending length of the pad-dry-cured cotton fabrics (Table **3**). Mainly, the padding procedure did not affect on air-permeability, but a slight decrease in flexibility of the treated cotton gauze samples was detected in warp/weft with raising the concentration of hydrazone-based probe. The durable performance of the treated cotton gauze to light, perspiration, wash and rub was explored. No changes were detected for the treated cotton after wash. In general, the fastness and photostability were satisfactory for all concentrations of the hydrazone-based dye as shown in Table **4**. However, a little decrease in the fastness and photostability was monitored upon increasing the hydrazone-based probe concentration.

Table 3: Bend-length and air-permeability of the treated gauze samples.

Dye wt%	Bend length (cm)		Air-permeability ($cm^3/cm^2/s^1$)
	Weft	*Wrap*	
Blank	2.26	2.85	82.49
0.5	2. 98	3.05	78.09
1.0	3.17	3.28	77.75
1.5	3.46	3.41	77.96
2.0	3.72	3.78	76.43
2.5	3.98	4.07	75.82

Table 4: Colorfastness properties of the pad-dry-cured fabrics.

Dye wt%	Wash		Perspiration				Rubbing		Light
	Alt.*	St.*	Acidic		Basic		Dry	Wet	
			Alt.*	St.*	Alt.*	St.*			
0.5	4-5	4-5	4	4	4-5	4-5	3-4	3-4	6
1.0	4-5	4-5	4	4	4-5	4-5	3-4	3-4	5-6
1.5	4	4	4	4	4	4	3-4	3	6
2.0	4	4	4	4	4	4	3-4	3	5-6
2.5	4	4	4	4	4	4	3	3	5-6

** Alt. = alteration in color; St. = staining on cotton.*

The reversibility of treated cotton gauze sample (1.5wt%) was explored after monitoring a wound mimic solution, the maximum absorbance wavelength were repeated back-and-forth as the fabric exhibited purple (535nm) color after exposure to wound mimic solution and orange color (450nm) after washing with distilled water and air-drying to remove the alkaline effect of the wound mimic solution. The absorbance wavelength was reported on Texflach ACS/Datacolor. This cycle of exposure to wound mimic solution followed by washing was repeated (Figure **2**) to indicate high stability.

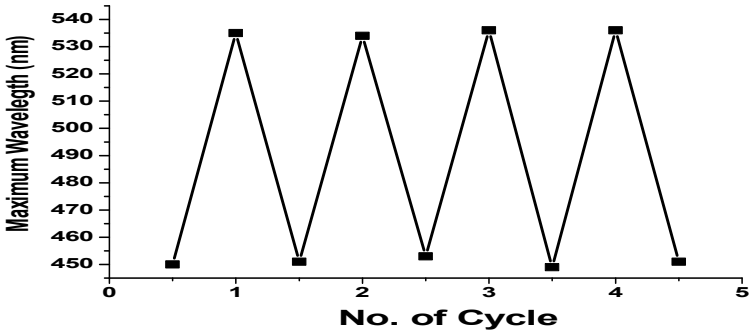

Figure 2: Changes in the absorbance wavelength (450nm for orange and 535nm for purple) of dip-coated (pad-dry-cured at room temperature) cotton fabric (Sample T_3).

4. Conclusion

Hydrazone disperse colorant with pH-sensing properties were prepared and applied to textile cotton gauze. The color change of the solid state textile gauze matrix was determined by the color coordinates as pH changes. The color of the treated textile gauze matrix was instantly changed from orange to purple in alkaline conditions. Microcapsules were assembled from a crosslinked Ca-alginate capsule shell integrated with hydrazone dye capsule core. Those microcapsules

were loaded on smart cotton gauze bandage to be applied for naked-eye wound pH monitoring depending on the color change of the deprotonated-protonated hydrazone dye from orange to purple associated with the medium pH from acidic to alkaline, respectively. The results were proved by exploring surface morphology and composition of the treated cotton gauze employing scanning electron microscopy, energy-dispersive X-ray, and mapping. The comfort properties of the treated cotton gauze samples were evaluated to show acceptable fastness, flexibility and breathability.

Acknowledgements

Technical support from National Research Centre, Cairo, Egypt; is gratefully acknowledged.

References

[1] Hu, Jinlian, Harper Meng, Guoqiang Li, and Samuel I. Ibekwe. "A review of stimuli-responsive polymers for smart textile applications." *Smart Materials and Structures* 21, no. 5 (2012): 053001.

[2] Stoppa, Matteo, and Alessandro Chiolerio. "Wearable electronics and smart textiles: a critical review." *sensors* 14, no. 7 (2014): 11957-11992.

[3] Cherenack, Kunigunde, Christoph Zysset, Thomas Kinkeldei, Niko Münzenrieder, and Gerhard Tröster. "Woven electronic fibers with sensing and display functions for smart textiles." *Advanced materials* 22, no. 45 (2010): 5178-5182.

[4] Cherenack, Kunigunde, and Liesbeth van Pieterson. "Smart textiles: Challenges and opportunities." *Journal of Applied Physics* 112, no. 9 (2012): 091301.

[5] Bedeloglu, Ayse, Ali Demir, Yalcin Bozkurt, and Niyazi Serdar Sariciftci. "A photovoltaic fiber design for smart textiles." *Textile Research Journal* 80, no. 11 (2010): 1065-1074.

[6] Schwarz, Anne, Lieva Van Langenhove, Philippe Guermonprez, and Denis Deguillemont. "A roadmap on smart textiles." *Textile progress* 42, no. 2 (2010): 99-180.

[7] Massaroni, Carlo, Paola Saccomandi, and Emiliano Schena. "Medical smart textiles based on fiber optic technology: an overview." *Journal of functional biomaterials* 6, no. 2 (2015): 204-221.

[8] Di, Jiangtao, Xiaohua Zhang, Zhenzhong Yong, Yongyi Zhang, Da Li, Ru Li, and Qingwen Li. "Carbon□Nanotube Fibers for Wearable Devices and Smart Textiles." Advanced materials 28, no. 47 (2016): 10529-10538.

[9] Little, Anna F., and Robert M. Christie. "Textile applications of photochromic dyes. Part 1: establishment of a methodology for evaluation of photochromic textiles using traditional colour measurement instrumentation." Coloration Technology 126, no. 3 (2010): 157-163.

[10] Feczkó, Tivadar, Krisztián Samu, Klára Wenzel, Branko Neral, and Bojana Voncina. "Textiles screen□printed with photochromic ethyl cellulose–spirooxazine composite nanoparticles." *Coloration Technology* 129, no. 1 (2013): 18-23.

[11] Morsümbül, S., and EP Akçakoca Kumbasar. "Photochromic textile materials." In *IOP Conference Series: Materials Science and Engineering*, vol. 459, no. 1, p. 012053. IOP Publishing, 2018.

[12] Valdés, Arantzazu, Marina Ramos, Ana Beltran, and Maria C. Garrigos. "Recent Trends in Microencapsulation for Smart and Active Innovative Textile Products." *Current Organic Chemistry* 22, no. 12 (2018): 1237-1248.

[13] Kennedy, J. F., K. Bunko, E. Santhini, Ketankumar Vadodaria, and S. Rajasekar. "The use of 'smart'textiles for wound care." In *Advanced textiles for wound care*, pp. 289-311. Woodhead Publishing, 2019.

[14] Vik, Michal, and Aravin Prince Periyasamy. *Chromic Materials: Fundamentals, Measurements, and Applications*. CRC Press, 2018.

[15] Horrocks, A. Richard, and Subhash C. Anand, eds. *Handbook of Technical Textiles: Technical Textile Applications*. Woodhead Publishing, 2016.

[16] Dreifke, Michael B., Amil A. Jayasuriya, and Ambalangodage C. Jayasuriya. "Current wound healing procedures and potential care." *Materials Science and Engineering: C* 48 (2015): 651-662.

[17] Melai, Bernardo, Pietro Salvo, Nicola Calisi, Letizia Moni, Andrea Bonini, Clara Paoletti, Tommaso Lomonaco, Vincenzo Mollica, Roger Fuoco, and Fabio Di Francesco. "A graphene oxide pH sensor for wound monitoring." In *2016 38th Annual International Conference of the IEEE Engineering in Medicine and Biology Society (EMBC)*, pp. 1898-1901. IEEE, 2016.

[18] Rahimi, Rahim, Manuel Ochoa, Tejasvi Parupudi, Xin Zhao, Iman K. Yazdi, Mehmet R. Dokmeci, Ali Tamayol, Ali Khademhosseini, and Babak Ziaie. "A low-cost flexible pH sensor array for wound assessment." *Sensors and Actuators B: Chemical* 229 (2016): 609-617.

[19] Milne, Stephen D., Ihab Seoudi, Hanadi Al Hamad, Talal K. Talal, Anzila A. Anoop, Niloofar Allahverdi, Zain Zakaria, Robert Menzies, and Patricia Connolly. "A wearable wound moisture sensor as an indicator for wound dressing change: an observational study of wound moisture and status." *International wound journal* 13, no. 6 (2016): 1309-1314.

[20] Liu, Xiyuan, and Peter B. Lillehoj. "Embroidered electrochemical sensors on gauze for rapid quantification of wound biomarkers." *Biosensors and Bioelectronics* 98 (2017): 189-194.

[21] Najafi, Bijan, Gurtej S. Grewal, Manish Bharara, Robert Menzies, Talal K. Talal, and David G. Armstrong. "Can't stand the pressure: the association between unprotected standing, walking, and wound healing in people with diabetes." *Journal of diabetes science and technology* 11, no. 4 (2017): 657-667.

[22] Sheybani, Roya, and Anita Shukla. "Highly sensitive label-free dual sensor array for rapid detection of wound bacteria." *Biosensors and Bioelectronics* 92 (2017): 425-433.

[23] McLister, Anna, Jolene McHugh, Jill Cundell, and James Davis. "New developments in smart bandage technologies for wound diagnostics." *Advanced Materials* 28, no. 27 (2016): 5732-5737.

[24] Wells, Michael C., Mark Parker, Daniel J. Clarius, Andrew Parker, Faraidoon Pundole, Tom Woods, and Mark Niederauer. "Apparatus and methods for controlling tissue oxygenation for wound healing and promoting tissue viability." U.S. Patent 9,730,838, issued August 15, 2017.

[25] Kassal, Petar, Jayoung Kim, Rajan Kumar, William R. de Araujo, Ivana Murković Steinberg, Matthew D. Steinberg, and Joseph Wang. "Smart bandage with wireless connectivity for uric acid biosensing as an indicator of wound status." *Electrochemistry Communications* 56 (2015): 6-10.

[26] Wahabzada, Mirwaes, Manuela Besser, Milad Khosravani, Matheus Thomas Kuska, Kristian Kersting, Anne-Katrin Mahlein, and Ewa Stürmer. "Monitoring wound healing in a 3D wound model by hyperspectral imaging and efficient clustering." *PloS one* 12, no. 12 (2017): e0186425.

[27] Jankowska, D. A., M. B. Bannwarth, C. Schulenburg, G. Faccio, K. Maniura-Weber, R. M. Rossi, L. Scherer, M. Richter, and L. F. Boesel. "Simultaneous detection of pH value and glucose concentrations for wound monitoring applications." *Biosensors and Bioelectronics* 87 (2017): 312-319.

[28] Ranieri, M., S. Klein, C. Taeger, A. Kotrade, M. Nerlich, J. Dolderer, L. Prantl, and S. Geis. "Transepidermal oxygen flux measurement–First clinical application for postoperative wound monitoring." *Clinical hemorheology and microcirculation* 66, no. 2 (2017): 175-182.

[29] McGilvray, Kirk C., Emre Unal, Kevin L. Troyer, Brandon G. Santoni, Ross H. Palmer, Jeremiah T. Easley, Hilmi Volkan Demir, and Christian M. Puttlitz. "Implantable microelectromechanical sensors for diagnostic monitoring and post□surgical prediction of bone fracture healing." Journal of Orthopaedic Research 33, no. 10 (2015): 1439-1446.

[30] Cui, Yao, Yu An, Tongyu Jin, Fan Zhang, and Pingang He. "Real-time monitoring of skin wound healing on nano-grooves topography using electric cell-substrate impedance sensing (ECIS)." *Sensors and Actuators B: Chemical* 250 (2017): 461-468.

[31] Mohr, Gerhard J., and Heidrun Müller. "Tailoring colour changes of optical sensor materials by combining indicator and inert dyes and their use in sensor layers, textiles and non-wovens." *Sensors and Actuators B: Chemical* 206 (2015): 788-793.

[32] DeRouin, Andrew J., Nina Pacella, Chunfeng Zhao, Kai-Nan An, and Keat Ghee Ong. "A Wireless Sensor for Real-Time Monitoring of Tensile Force on Sutured Wound Sites." *IEEE Trans. Biomed. Engineering* 63, no. 8 (2016): 1665-1671.

[33] Roca, Joan, Miquel Nogués, Rafael Villalobos, María Carmen Mías, Martí Comellas, Cristina Gas, and Jorge Juan Olsina. "Surgical dynamometer to simultaneously measure the tension forces and the distance between wound edges during the closure of a laparotomy." *Sensors* 18, no. 1 (2018): 189.

[34] Khattab, Tawfik A., Hussein Abou-Yousef, and Samir Kamel. "Photoluminescent spray-coated paper sheet: Write-in-the-dark." *Carbohydrate polymers* 200 (2018): 154-161.

[35] Khattab, Tawfik A., Ahmed A. Allam, Sarah I. Othman, May Bin-Jumah, Hanan M. Al-Harbi, and Moustafa M. G. Fouda. "Synthesis, Solvatochromic Performance, pH Sensing, Dyeing Ability, and Antimicrobial Activity of Novel Hydrazone Dyestuffs" *Journal of Chemistry* (2019). Doi: 10.1155/2019/7814179

ضمادة ذكية مصبوغة بصبغة استشعار مغلفة بألجينات الكالسيوم لرصد التئام الجروح

[3] – نسرين عوض النقيب[2]* – أحمد محمد فاروق أحمد[1]توفيق خطاب

[١] قسم الصباغة والطباعة والمواد الوسيطة – شعبة بحوث الصناعات النسيجية – المركز القومي للبحوث – مصر

[٢] قسم الاقتصاد المنزلي – كليه التربية النوعية – جامعة الفيوم – مصر

[٣] قسم اقتصاد منزلي (ملابس ونسيج) كلية البنات – جامعة عين شمس – مصر

الملخص العربي

تم تطوير ضمادة ذكية لمتابعة التئام الجروح ، وذلك اعتمادا علي تغير اللون عند التئام الجروح. يمكن أن يؤدي تطوير اداة استشعار لدرجة الحموضة بالتقنية اللونية النسيجية إلى استخدام تطبيقات فعالة ، حيث أنه يمثل إمكانية متابعة الاس الهيدروجيني بطريقة سريعة باستخدام خامة رخيصة ومرنة. تم تحضير صبغة التراي سيانوهيدرازون واستخدامها كمادة استشعار لدرجة الحموضة والقاعدية. حيث تم تغليف صبغة التراي سيانوهيدرازون المتجاوبة لدرجة الاس الهيدروجيني كمادة داخلية والجينات الكالسيوم كجدار خارجي للكبسولة ، والتي تم تحميلها على شاش قطني بطريقة الغمر. هذه التغيرات في اللون القابل لاعادة الاستخدام والتي تتجاوب مع تغيرات الأس الهيدروجيني كانت نتيجة لتخليق الشحنة الاليكترونية العالية لمركب التراي سيانوهيدرازون أنيون المنتج الذي يؤدي إلى انتاج جزيء من نوع الكوينويد حيث تم استخدام هذا الملون في المواد النسيجية التقنية لاكسابها القدرة على استشعار الرقم الهيدروجيني. اعتمد النهج المعتمد في هذه الدراسة على صباغة القطن الشاش باستخدام صبغة التراي سيانوهيدرازون محملة داخل كابسولات الكالسيوم الجينات لمتابعة التئام الجروح. أظهر الشاش المصبوغة تغيرًا واضحًا في اللون عند التعرض لمحاليل قاعدية وحمضية كما هو موضح بإحداثيات اللون. تشير نتائجنا إلى تغير واضح في اللون يظهر بالعين المجردة ، من اللون البرتقالي إلى اللون الأرجواني ، والتي يمكن التعرف عليها على سطح الأقمشة المستخدمة. تم دراسة التشكل السطحي وتكوين الشاش القطني المعالج تحت المجهر الإلكتروني الماسح الضوئي ، الأشعة السينية المشتتة للطاقة ، ورسم الخرائط العنصري. تمت دراسة الشاش القطني المعالج من خلال استكشاف نفاذية الهواء ، والصلابة ، وثبات اللون.